



Some properties of the lower electronic states for nonlinear He 3 + clusters

F. A. Gianturco, M. P. de Lara-Castells, and F. Schneider

Citation: *The Journal of Chemical Physics* **107**, 1522 (1997); doi: 10.1063/1.474522

View online: <http://dx.doi.org/10.1063/1.474522>

View Table of Contents: <http://scitation.aip.org/content/aip/journal/jcp/107/5?ver=pdfcov>

Published by the [AIP Publishing](#)

Articles you may be interested in

[Spectroscopic properties of novel aromatic metal clusters: NaM 4 \(M = Al,Ga,In \) and their cations and anions](#)
J. Chem. Phys. **120**, 10501 (2004); 10.1063/1.1738112

[An ab initio, analytically fitted, global potential energy surface for the ground electronic state of He 3 +](#)
J. Chem. Phys. **119**, 4694 (2003); 10.1063/1.1594711

[Geometries and spectroscopic properties of silicon clusters \(Si 5 , Si 5 + , Si 5 - , Si 6 , Si 6 + , and Si 6 - \)](#)
J. Chem. Phys. **116**, 3690 (2002); 10.1063/1.1446027

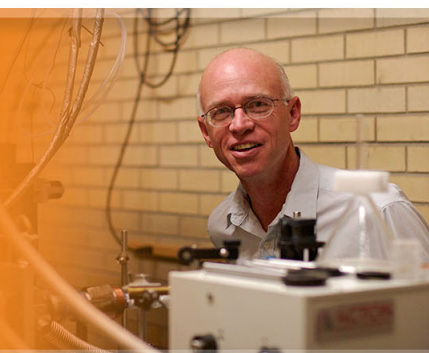
[Geometries and spectroscopic properties of germanium and tin hexamers \(Ge 6 ,Ge 6 + ,Ge 6 - ,Sn 6 ,Sn 6 + , and Sn 6 - \)](#)
J. Chem. Phys. **115**, 3121 (2001); 10.1063/1.1386795

[Short-time charge motion in He n + clusters](#)
J. Chem. Phys. **109**, 10873 (1998); 10.1063/1.477784

The logo for AIP Applied Physics Letters. It features the letters 'AIP' in a large, white, sans-serif font on the left, followed by a vertical bar and the text 'Applied Physics Letters' in a smaller, white, sans-serif font on the right. The background is a solid orange color.

AIP | Applied Physics
Letters

is pleased to announce **Reuben Collins**
as its new Editor-in-Chief



Some properties of the lower electronic states for nonlinear He₃⁺ clusters

F. A. Gianturco

Max-Planck-Institut für Strömungsforschung, Bunsenstr. 10, 37073 Göttingen, Germany,
and Department of Chemistry,^{a)} The University of Rome, Città Universitaria, 00185 Rome, Italy

M. P. de Lara-Castells

Department of Chemistry, The University of Rome, Città Universitaria, 00185 Rome, Italy, and Instituto de Matemáticas y Física Fundamental,^{a)} C.S.I.C., Serrano 123, 28026, Madrid, Spain

F. Schneider

Department of Chemistry, The University of Rome, Città Universitaria, 00185 Rome, Italy,
and Toblacherstr. 42^{a)} Berlin Pankow 13187, Germany

(Received 25 September 1996; accepted 23 April 1997)

Accurate, highly correlated calculations have been carried out for the ground electronic state and for a few of the lower excited electronic states, two of which are discussed in this work, of the trimer ionic helium cluster. Both linear asymmetric and nonlinear, symmetric, and asymmetric, configurations have been considered over a rather broad range of nuclear geometries. The results confirm the experimentally found [Chem. Phys. **102**, 2773 (1995)] fragmentation patterns involving He and He⁺ fragments only and further suggest a range of possible nuclear geometries from which nonadiabatic couplings could also lead to He₂⁺ fragments, albeit with a lower probability than the former channels. © 1997 American Institute of Physics. [S0021-9606(97)00929-X]

I. INTRODUCTION

The ionized clusters of helium atoms, especially for small values of the number n of a monomer rare gas, are among the simplest of the increasing number of cluster ions that have recently attracted a great deal of attention from a broad variety of experiments and of theoretical methods.¹⁻³ When one considers the energetically most favored structures of the smaller ionized helium clusters, He _{n} ⁺ with n from 3 to 7, one finds for instance, that a linear trimer molecule constitutes its ionic core⁴⁻⁶ and is surrounded by an equatorial ring of neutral atoms. So the qualitative picture of the binding structure is one in which the core trimer carries the positive charge and has its three atoms covalently bound to each other, while the atoms further in the ring are mainly bound by the weaker polarization forces. We recently carried out further calculations using a Local Density Approximation (LDA) method to treat correlation effects⁷ and found a general confirmation of such a picture for the binding scheme of ionic clusters up to $n = 7$.

The dynamical behavior of such simple clusters is also of interest in order to establish even more in detail their general fragmentation patterns and the preferential pathways for energy redistribution that lead to these patterns.⁸ We have recently analyzed the nature of the electronic excitation process of the linear helium trimer, in a symmetric configuration of its ion,⁹ and found that the behavior of the charge relocation after electronic excitation can explain the appearance of the various peaks observed in the time-of-flight experimental spectra⁸ and can help us to understand the relative stability of the fragmentation species.

In a more general analysis of both the ground and the excited electronic states, however, one needs to further probe

other arrangements and to see the possible effects of bent structure formation during the ionic cluster breakup process. The object of the present study is precisely that of presenting a fairly detailed analysis, from highly correlated *ab initio* calculations, of the possible fragmentation pathways for various types of distorted nuclear structures other than the linear symmetric arrangement discussed earlier.⁹

II. THE COMPUTATIONAL DETAILS

The present set of calculations was carried out using highly correlated wave functions via the Multireference single and Double Excitations with Configuration Interaction (MRD-CI) method described many times before,¹⁰⁻¹³ and used previously by us on similar problems:^{14,15} thus, its detailed computational aspects will not be repeated here. The basis set chosen was the cc-pVTZ (correlation consistent polarized valence triple zeta) suggested earlier by Dunning.¹⁶ The atomic basis set employed in it was the $6s2p1d$ contracted to $3s2p1d$, which leads to 45 contracted GTO functions for the He₃⁺ system. The doublet, open-shell SCF occupation was given by $(1\sigma_g)^2(1\sigma_n^2)(2\sigma_g^2)$ in the $C_{\infty v}$ arrangement and all 45 SCF-MOs were used in the CI procedure.

In a typical run, about 18–26 optimized main configurations were used to generate 20 000–30 000 singly and doubly excited configurations out of which 15 000 were then selected by adopting a threshold of 0.02–0.05 μ hartree. The ensuing CI extrapolation gave rise only to corrections of about 0.001 a.u. to the lower roots.

The final Hamiltonian matrix in the selected configuration space was then diagonalized to yield five to seven roots, and the final wave functions turned out to be represented by the reference configurations with rather high accuracy since

^{a)}Present address.

the relevant coefficient weights (the $c^* \times c$ quantities) summed up to values of 0.98–0.99.

We considered a variety of geometric arrangements in order to complement what had been already obtained in the symmetric linear breakup discussed earlier.⁹ Thus, we generated the linear asymmetric breakup with the two bond distances R_1 and R_2 different from each other; then the helium insertion process of the C_{2v} arrangement. In the latter instance the two considered distances were the ionic diatom bond, r , and the third helium distance from the midpoint of the latter, i.e., the R distance perpendicular to the diatomic system (see below). Finally, we also considered the coordinates of an arbitrary bent structure, whereby the (He–He)⁺ bond distance, r , and the distance of its midpoint to the third atom, R , formed a fixed angle = 60°, and the relevant electronic states then belong to the C_s symmetry. Each of the radial distances, in all cases examined, were extended up to $6.0a_0$ by intervals varying between 0.15 and $0.5a_0$ from the region of minimum energy of the linear trimer ion. In the linear arrangements, a total of 120 actually computed points was employed to generate the maps discussed below. In the C_s arrangement a total of 270 points was generated, while in the C_{2v} arrangement 120 points were also computed. Finally, other orientations were also computed for the Jacobi angle, from 10° to 60° with intervals of 10°, for a total of 500 points.

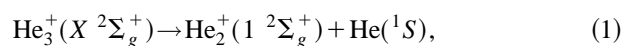
III. DISCUSSION OF RESULTS

In the previous calculations of the equilibrium structure of the He₃⁺ species⁹ we found an optimized symmetric equilibrium geometry with $R = 2.34a_0$ in each bond, a result that compared well with the best-known theoretical value from CEPA-SD calculations⁵ of $2.35a_0$. Furthermore, the symmetric dissociation energy into He⁺+He+He was found to be 2.59 eV, also in good accord with the earlier value of 2.58 eV from Ref. 5.

A. The linear configurations

The more extensive calculations of the asymmetric dissociation process are now shown on the left side of Fig. 1, where we report the lowest three roots (bottom to top) for the collinear configurations. They correspond to the $^2\Sigma^+$ potential energy surfaces (PES) associated to the ground electronic state and the first two excited electronic states of the He₃⁺ ion already discussed by us.⁹ Only the ground-state symmetry, $1^2\Sigma^+$, shows the existence of a basin where bound trimers clusters are located, while the next two electronic states are repulsive at all geometries within the relevant region of interaction, and therefore possible electronic excitations of the bound trimer must lead to its full dissociation when such states are reached in the excitation process, in complete analogy to what happens for the case of linear symmetric arrangements.^{8,9}

Along either of the shown coordinates, R_1 and R_2 , one can also follow adiabatically the ground electronic PES only and therefore reach the partial dissociative channel,



which asymptotically leads to a helium dimer ion equilibrium geometry of $2.041a_0$ and a binding energy of 2.4–2.5 eV, while the third helium atom dissociates with an extra energy of 0.15–0.17 eV.¹⁷ Thus, the collinear calculations indicate the following.

(i) That to excite the linear trimer into either of its lower electronic states leads to a full fragmentation of it, independently of the chosen initial geometry, i.e. both from its basin of minimum energy and from any asymmetrically stretched configuration.

(ii) That the ground state electronic potential can lead to adiabatic dissociation of the cluster either into three fragments or into a dimer ion plus a neutral atom.

(iii) That the symmetric stretch process is connected to a first excited electronic state of $1^2\Sigma_u^+$ symmetry, which is reached by optically allowed transitions from the symmetric ground state of the trimer ion.⁹

Our previous calculations⁹ also showed that the ground electronic state of the trimer ions has a positive charge distributed over the three-center system when close to its equilibrium geometry at the center of the basin and that such a charge migrates out to the two wing atoms as symmetric stretching deformation is undergone by the molecule. We could therefore confirm the qualitative reasoning given from experiments⁸ that the dramatic difference of excitation energies between the dimer ion (~ 10 eV) and the trimer symmetric ion (5.34 eV) is related to the existence of a different chromophore in the latter species. Thus, the simpler alternative structure consisting of a dimer ion core with a loosely attached neutral atom should be ruled out for the trimeric cluster in its ground state equilibrium geometry. On the other hand, the present extension of the calculations to the asymmetric stretch configurations indicates clearly that the removal of only one of the wing helium atoms from the trimer does lead to a stabilization of the charge on the remaining dimer and therefore to possible, highly deformed linear structures that correspond to a dimeric ionic core loosely attached to a neutral He atom. However, the experimental evidence indicates that the trimer formation after the initial supersonic expansion, followed by ionization via electron impact, is most likely to occur with the production of a vibrationally “cold” symmetric trimer ions where the chromophore acting during the ensuing laser excitation is then clearly represented by the new He₃⁺ structure and not by a simpler dimeric ion core to which the third He atom is attached. Another, interesting experimental result showed that the product time-of-flight spectra of He₃⁺ contain peaks related to one fast neutral He atom, to one fast ionic He⁺ and to a third slow neutral He atom.⁸ This pattern was explained by our calculations when we examined the linear symmetric dissociative path,⁹ and where we showed that the relevant excited electronic state, which can be reached via a dipole-allowed transition ($1^2\Sigma_u^+ \leftarrow X^2\Sigma_g^+$) yields a modified electronic density distribution where the positive charge now resides on one of the two wing He atoms, even for cluster geometries still within the Frank–Condon (FC) region of the Franck–Condon ground electronic configuration. Thus, it can create a fast ionic and a fast neutral fragment, together

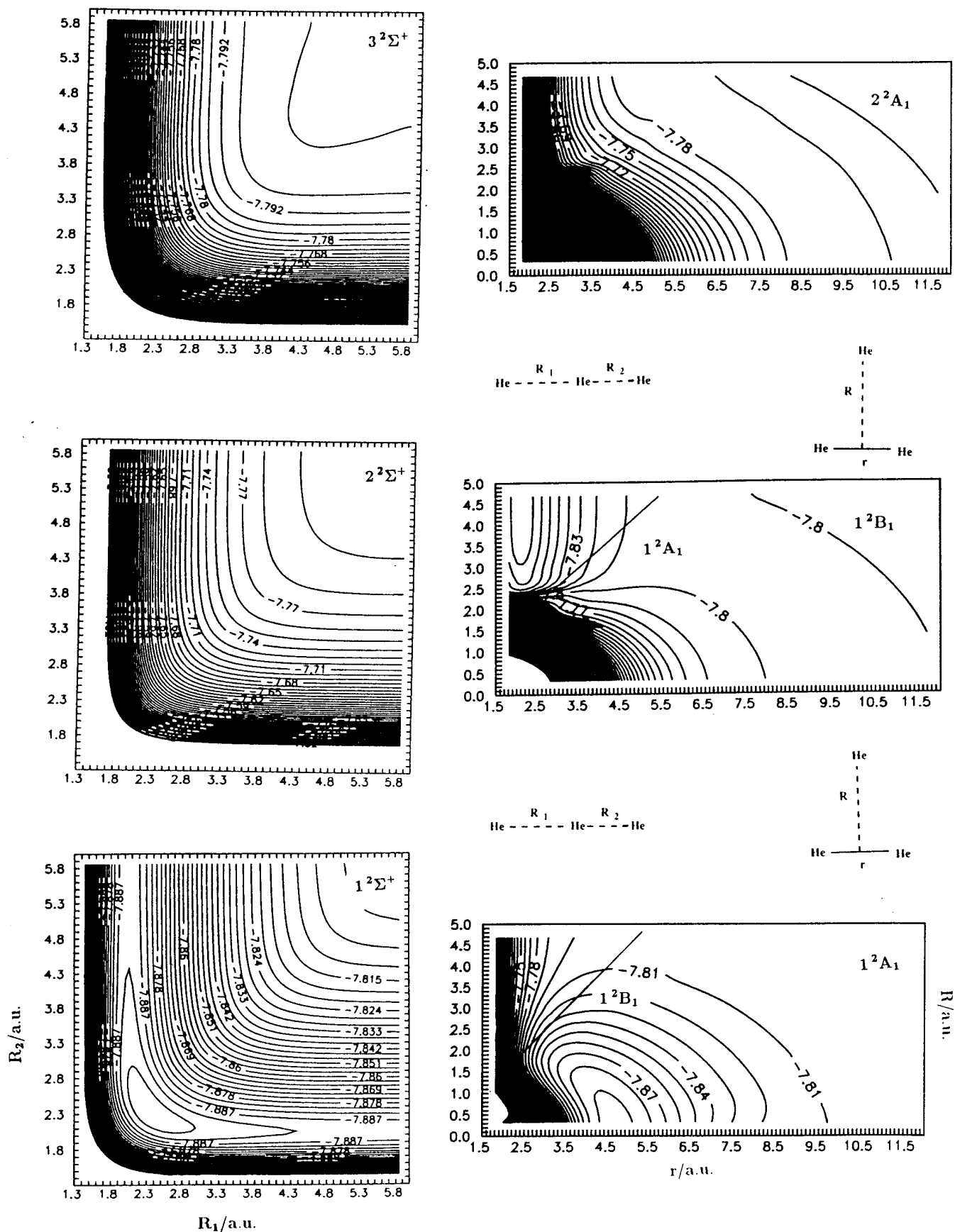


FIG. 1. Computed MRD-CI potential energy surfaces for different He₃⁺ geometries. Left column diagrams: The first three lower electronic states (bottom to top) for the linear arrangements. Right column diagrams: The first three lower electronic states (bottom to top) for the C_{2v} nonlinear arrangements. The radial coordinates are defined for the two arrangements on the right side of the figure.

with a slow neutral signal from the central helium atom as the system breaks up symmetrically along such a reaction coordinate, as seen in the experiments.⁸ It therefore becomes of interest to further find out if other nuclear regions of the relevant PES still support this explanation and what is the possible role played by bent structures of the trimer ions in case they happen to be formed during the ionic cluster preparation after supersonic expansion.

B. The bent configurations

The investigation of the asymmetric stretch motion, as mentioned before, indicates that the removal of one helium atom preferentially transfers the charge on the residual dimer ion when the breakup occurs adiabatically on the lowest PES (the bottom left of Fig. 1). However, when excitation occurs to the next lowest-energy surface ($2^2\Sigma^+$), then the fragmentation process is dissociative for all linear arrangements, and the ensuing charge migration produces the various fragments, as indicated by experiments.⁸

If we now consider a specific bent structure, i.e., the one given by a value of 60° for the Jacobi angular coordinate of the He_3^+ system (see Fig. 2), we can further analyze the possible effects of nonlinear configurations on the fragmentation process. Large values of the R coordinate thus correspond to the third He atom being far away from the residual dimer, which is now given by the He_2^+ ion, as one can see from the diagram on the lower-left side of Fig. 2. Hence, bent structures with a strongly asymmetric stretched configuration give rise, in their ground electronic state, $^2A'$, to a loosely bound He atom and a dimer ionic core. On the other hand, as the R coordinate becomes smaller is now the other internuclear distance that tends to stretch, and we simply see the insertion of the third He atom to form He_3^+ in its equilibrium configuration: the minimum in the same lower-left plot of Fig. 2 is, in fact, now located, for $R \sim 0$, at a value of $\sim 4.68a_0$ for the r coordinate. Thus, we can say that the possible bent structures of the trimer ion, when considered in their ground electronic state, behave very similarly to the ground state of the linear configurations, in the sense that can adiabatically break up into He_2^+ and He fragments or into $\text{He}+\text{He}+\text{He}^+$ fragments.

If we now consider the next two excited electronic states, the ones already considered⁹ for the excitation process of the linear configuration, we obtain the results shown on the upper part of Fig. 2. We show there, in fact, the next C_s excited state, $2^2A'$, on the left side and the third electronic state, $3^2A'$, on the upper right side of the same figure. We clearly see that both electronic states exhibit a marked repulsive behaviour for all geometries and for the whole grid of (R, r) values examined in our work. The results therefore indicate that the excitation process carried out during the experimental analysis⁸ could only produce a breakup pattern of three particles, one ionic and two neutral ones, if it were to occur from an initial He_3^+ cluster given by the above bent configuration. This is just what it did when the linear configuration of the cluster was considered before, and therefore we can say that the results given by the sym-

metric breakup path are confirmed by these additional calculations. We will further show below, however, how the situation could change when a more symmetric bent structure is considered for the cluster ion and when a third option is examined as a possible, nuclear excited structure of the initial, ionized trimer cluster.

C. The C_{2v} configurations

So far the results of our correlated calculations indicate that both linear, symmetric and asymmetric, and the C_s nonlinear structures of the trimer ion, yield a similar breakup pattern on electronic excitation, one that agrees with the results found experimentally from the time-of-flight spectra.⁸

Let us now consider the triangular, C_{2v} , structure whereby the coordinate R describes the ‘‘insertion’’ of a third He atom into the helium dimer taken at a given relative distance r . The behavior of the three lowest electronic energy surfaces is shown, bottom to top, on the right side of Fig. 1. When we examine the lowest two electronic PES, the 1^2A_1 and the 1^2B_1 , we see immediately that these two surfaces cross for a set of coordinate values shown by a solid straight line in both the lowest and the middle diagrams of Fig. 1. Furthermore, we see that the triangular structure is an excited configuration with respect to the linear symmetric structure and that it can reach the latter minimum for $R \sim 0$ and $r \sim 4.68a_0$, as expected. If one now adiabatically remains on the 1^2A_1 potential surface, however, one sees that the removal of the third helium atom from the ionic dimer leads to an excited state where the system breaks up into $\text{He}+\text{He}+\text{He}^+$, while the crossing with the 1^2B_1 state leads, over a small barrier, to the formation of He_2^++He as an alternative final product from fragmentation, as shown by the middle diagram on the right side of Fig. 1. This indicates that nonadiabatic coupling between the two electronic states could lead the system to evolve into either of the above channels after being formed in the most stable linear, symmetric structure given by the basin of energy in the bottom diagram of Fig. 1 (right-hand side). When carrying out the electronic excitation process experimentally, the initially linear symmetric lowest-energy structure of the trimer cluster is first excited by a selected laser wavelength between $\lambda = 310\text{--}300$ nm and subsequently extracted into a second linear time-of-flight, mass-selection spectrometer.⁸ The excitation then could bring the system into the Franck–Condon (FC) region of the 1^2B_1 electronic state, which is seen from Fig. 1 to be fully dissociative to $\text{He}+\text{He}+\text{He}^+$. However, if the system has enough time to move across the seam that exists with the lower 1^2A_1 state (at a different geometry of the nuclei), then the possibility arises for it to dissociate into He_2^++He , as shown by the middle diagram and the right-hand side of Fig. 1.

D. The overall view

With the help of extensive, highly correlated *ab initio* calculations, we have examined the lowest three roots and the overall shapes of the corresponding PES that could give us information on the likely fragmentation patterns of helium

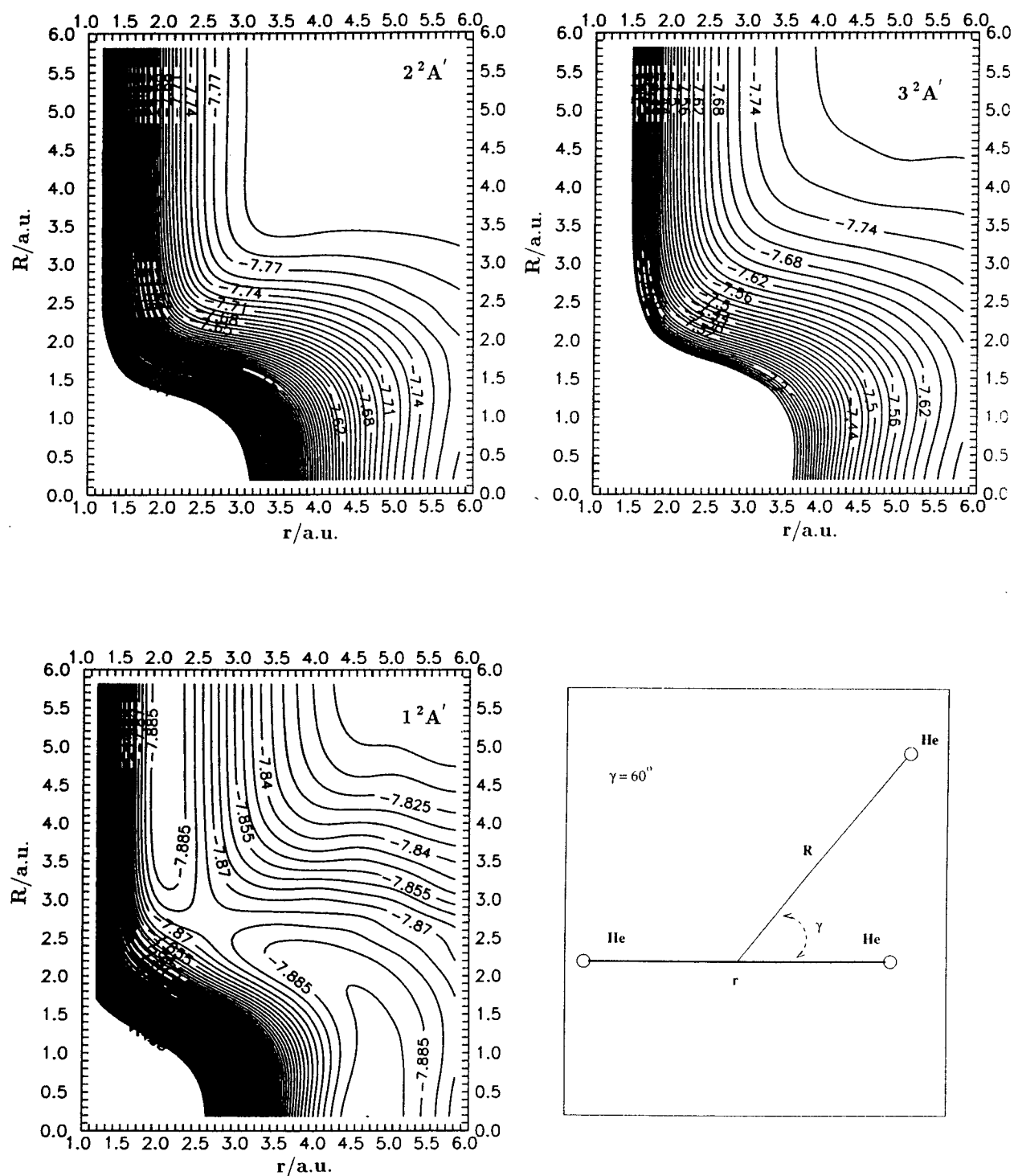


FIG. 2. Nonlinear C_s arrangement for the PES calculations of the lowest three electronic states. The states are defined, in increasing order of energy, from the lower left to the upper right. The geometry is given in the lower-right side of the figure.

trimer ions after they undergo electronic excitation to their first, dipole allowed, electronically excited state. The scope of the present computations was to cast more light on the possible role of nonlinear structures to provide breakup channels that may differ from the ones experimentally observed as dominant, i.e. the full dissociation channel into He+He+He⁺ fragments.⁸ The results of the present ap-

proach are summarized pictorially in Fig. 3 in order to provide a more immediate representation of the fragmentation paths.

We report in that figure the behavior of a reaction coordinate (S) for the two lowest electronic states involved in each of the three arrangements discussed in the previous section. The coordinate in question follows the minimum energy

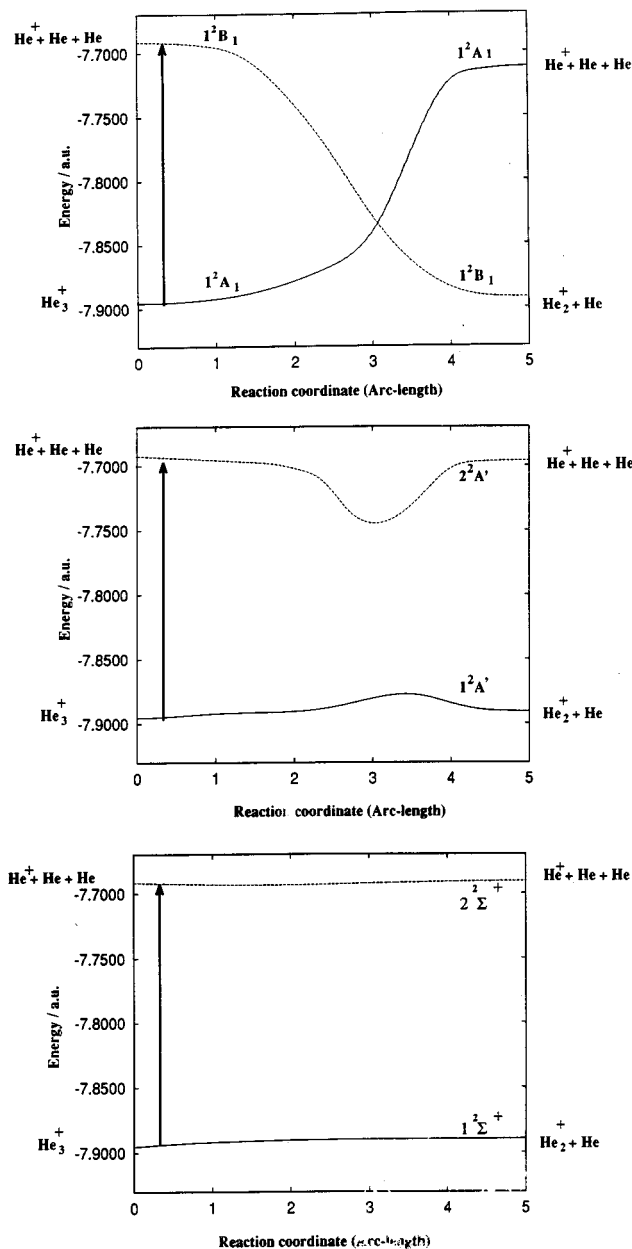


FIG. 3. Behavior of the computed lower two electronic PES for the three different arrangements discussed in this work. The energy profiles are shown along the reaction coordinate discussed in Eq. (2) of the main text. Lowest diagram: linear arrangement. Middle diagram: C_s arrangement. Top diagram: C_{2v} arrangement. The fragments listed outside the diagrams, left and right, refer to the initial and to the asymptotic channel compositions.

path in going from the one system configuration where one of the two radial variables is the smaller to another arrangement where the other variable has now become smaller. In particular, the three arrangements define their corresponding coordinates as follows:

$$S = \sqrt{(x - x_e)^2 + (y - y_e)^2}. \quad (2)$$

In the linear arrangement the values of $x_e = y_e = 2.34a_0$ are used, with x and y corresponding to the $\{R_1, R_2\}$ coordinates of Fig. 1. In the C_s arrangement, $x_e = 4.68a_0$, while $y_e = 0$ and the $\{x, y\}$ set corresponds to $\{r, R\}$, respectively. Finally,

the perpendicular arrangement of the C_{2v} geometry also uses $x_e = 4.68a_0$ and $y_e = 0$, while its radial Jacobi coordinates $\{r, R\}$ were used to represent the $\{x, y\}$ set required in Eq. (2).

In the case of the linear arrangement shown in the lowest diagram reported in Fig. 3, we have chosen as a reaction coordinate the half-region of the PES of Fig. 1, which goes from the minimum trimer configuration out to the asymptotic region for the asymmetric stretching. Furthermore, the two curves reported in Fig. 3 for the linear arrangements also have their asymptotic fragments listed outside the diagram, as it occurs with all the three diagrams shown in that figure. Thus, we see that the reaction coordinate for the asymmetric stretching motion on the ground electronic PES produces, as mentioned before, $\text{He} + \text{He}_2^+$ as the breakup asymptotic channel if the process remains adiabatically on that electronic surface. On the other hand, when the laser excitation brings the system up to its first excited state, the $2^2\Sigma^+$ electronic PES, the PES from our calculations shows that the system becomes fully dissociative at all geometries and invariably breaks up into $\text{He} + \text{He} + \text{He}^+$ after excitation, as seen in the experiments.

If we now consider the nonlinear structure of an arbitrary C_s symmetry, as reported in the middle diagram of Fig. 3, we see that the description of the fragmentation process remains largely similar to the linear case: The ground state reaction coordinate now goes from the region of $R \sim 0$ (in the PES of Fig. 2), where the ‘‘insertion’’ of a third He atom creates the minimum configuration of a linear He_3^+ , to the larger S values where $R \gg r$, with the latter being near the equilibrium value of He_2^+ and therefore producing the same breakup pattern, as in the case of the asymmetric linear stretch shown on the lower diagram of Fig. 3.

Here again we notice that the adiabatic process does not produce the experimentally observed fragmentation, while the excitation into the next higher electronic state (the $2^2A'$ state of the nonlinear trimer ion) shows once more the breakup species observed by experiments and also surmised by the previous calculations on the linear trimeric cluster. Thus, we can definitely say that possible deformations of the most stable geometry of the He_3^+ system reached after neutral cluster ionization, i.e., the symmetric linear geometry, do not change the outcomes of the fragmentation pattern after laser excitation of the ionic cluster.

It is interesting to note at this point that the change in energy when going from the linear to the bent structure is considerably small, thus indicating that the He_3^+ cluster is a rather floppy system with respect to bending motion and that the s orbitals involved in the bonding do not provide strong orientational forces. Furthermore, the internal angle used within the C_s geometry examined here is about 100° , which corresponds to an excited bending mode and that could, under fragmentation, increase the relative velocity of the neutral central atom with respect to the center of mass. This means that, according to the present computational results, both the linear and the nonlinear structures could originate from fragments with different velocities and therefore could give rise to a broader velocity distribution of the neutral peak

than that given by the other two peaks. It is reassuring to see that such velocity broadening is indeed experimentally observed for the trimer ion fragmentation⁸ and appears to confirm the reliability of the present calculations.

We can now turn to the special configuration given by the triangular structure of C_{2v} geometry, the one for which the computed PES are shown in Fig. 1 and have been already discussed in the previous section. The behavior of the reaction coordinate is shown by the top diagram of Fig. 3: both adiabatic paths are reported for the 1^2A_1 symmetry (the lower symmetry in the region of the linear trimer) and the 1^2B_1 symmetry that provides the energetically lower surface in the region where the third He atom is farther than $3.0a_0$ from the dimer ion center of mass. The crossing between minimum-energy paths is also clearly visible and indicates that after excitation in the FC region of the initial stable trimer, the system could evolve nonadiabatically to yield fragmentation into the dimeric ion and the neutral He atom. Such a transition, however, requires both a strongly deformed nonlinear trimer ion and no coupling between the two PES in the limited spatial region where the seam exists. Such features are obviously not greatly favored and may explain why no experimental observation of this fragmentation channel seems to exist.⁸ However, it is still interesting to observe that the calculations suggest such an option and that one may thus consider possible experimental arrangements, where this much weaker fragmentation channel could be detected.

IV. CONCLUSIONS

The rather extensive calculations of the present work indicate clearly that the charge migration mechanism after laser light excitation of the initial trimer into a repulsive PES still provides the basic explanation for the experimental findings. It has been verified by our present computations to be valid not only for breakup processes from linear cluster arrangements, both symmetric and asymmetric, but also for breakup channels originating from nonlinear arrangements of the cluster ion. Our present results also suggest that the possibility exists, if certain regions of phase space are reached by nuclear geometries, that the system is kept on a $2B_1$ electronic PES, which could provide a different fragmentation pattern after the primary laser excitation process. However, if one considers the rather limited region of nuclear geometries involved and the possibly low efficiency of the coupling between the two PES, it is still an open question if any experimental setup could detect the presence of this additional channel given the expected low intensity of the product

peaks. It is therefore fair to conclude from the present study that the full fragmentation of the trimer into atomic fragments (neutral and ionic) is the most likely occurrence in the experiments.

The present calculations on the trimer cluster therefore indicate that a great deal of information, which can explain several features of the time-of-flight experiments, could be gleaned by a detailed *ab initio* study of large regions of the involved PES of such highly quantum systems.

The actual values of the computed PES points are available via the EPAPS FTP server.¹⁸

ACKNOWLEDGMENTS

The financial support of the Italian National Research Council (CNR) and the Italian Ministry for Research and Technology (MURST) is acknowledged. M. P. de L.-C. thanks the EU for a COST visiting fellowship to the University of Rome under Project No. D3-0005/94. F.S. also thanks the EU for the award of a Fellowship (Cat. 30) under Contract No. ERB-CHBG-CT 9 303 46. Finally F.A.G. thanks the von Humboldt Stiftung for the award of a Senior Fellowship and Professor Peter Toennies for his warm hospitality in his laboratory in Gottingen, where this work was completed.

¹ *Clusters of Atoms and Molecules*, edited by H. Haberland (Springer, Berlin, 1994), Vols. I and II.

² U. Buck and H. Meyer, *Surf. Sci.* **156**, 275 (1985).

³ T. D. Märk, *Int. J. Mass Spectrom. Ion Phys.* **79**, 1 (1987).

⁴ J. Ackermann and H. Hogreve, *Chem. Phys.* **157**, 75 (1991).

⁵ V. Staemmler, *Z. Phys. D* **16**, 219 (1990).

⁶ V. Staemmler, *Z. Phys. D* **22**, 741 (1992).

⁷ P. de Lara-Castells and F. A. Gianturco, *Int. J. Quantum Chem.* **60**, 593 (1996).

⁸ H. Haberland, B. v. Issendorff, R. Fröchtenicht, and J. P. Toennies, *J. Chem. Phys.* **102**, 8773 (1995).

⁹ E. Buonomo, F. A. Gianturco, F. Schneider, P. de Lara-Castells, G. Delgado-Barrio, S. Miret-Arrés, and P. Villarreal, *Chem. Phys. Lett.* **259**, 641 (1996).

¹⁰ R. J. Buenker and S. D. Peyerimhoff, *Theor. Chim. Acta* **35**, 33 (1974).

¹¹ R. J. Buenker and S. D. Peyerimhoff, *Theor. Chim. Acta* **39**, 217 (1975).

¹² R. J. Buenker, S. D. Peyerimhoff, and W. Butscher, *Mol. Phys.* **35**, 171 (1978).

¹³ P. J. Bruna, S. D. Peyerimhoff, and R. J. Buenker, *Chem. Phys. Lett.* **72**, 278 (1980).

¹⁴ F. A. Gianturco and F. Schneider, *J. Phys. B* **29**, 1175 (1996).

¹⁵ F. A. Gianturco, S. Kumar, and F. Schneider, *J. Chem. Phys.* **105**, 156 (1996).

¹⁶ T. H. Dunning, *J. Chem. Phys.* **90**, 479 (1989).

¹⁷ M. Rosi and Ch. W. Bauschlicher, *Chem. Phys. Lett.* **159**, 479 (1989).

¹⁸ See AIP Document No. E-PAPS: **E-JCPA-107-1522** for 9 files of 54 KB total, which report the lowest three electronic states for each of the three orientations discussed in the paper. E-PAPS document files may be retrieved free of charge from our FTP server (<http://www.aip.org/epaps/epaps.html>) or from <ftp.aip.org> in the directory /epaps/. For further information: e-mail: paps@aip.org or fax: 516-576-2223.